Docosahexaenoic acid phospholipid differentially modulates the conformation of G90V and N55K rhodopsin mutants associated with retinitis pigmentosa

Xiaoyun Dong, María Guadalupe Herrera-Hernández, Eva Ramon, Pere Garriga

PII: S0005-2736(17)30060-3
DOI: doi:10.1016/j.bbamem.2017.02.006
Reference: BBAMEM 82425

To appear in: *BBA - Biomembranes*

Received date: 13 July 2016
Revised date: 9 February 2017
Accepted date: 11 February 2017

Please cite this article as: Xiaoyun Dong, María Guadalupe Herrera-Hernández, Eva Ramon, Pere Garriga, Docosahexaenoic acid phospholipid differentially modulates the conformation of G90V and N55K rhodopsin mutants associated with retinitis pigmentosa, *BBA - Biomembranes* (2017), doi:10.1016/j.bbamem.2017.02.006

Docosahexaenoic acid phospholipid differentially modulates the conformation of G90V and N55K rhodopsin mutants associated with retinitis pigmentosa

Xiaoyun Dong[1, †], María Guadalupe Herrera-Hernández[1, ‡], Eva Ramon[1], and Pere Garriga[1*]

[1]Grup de Biotecnologia Molecular i Industrial, Centre de Biotecnologia Molecular, Departament d'Enginyeria Química, Universitat Politècnica de Catalunya, Edifici Gaia, Rambla de Sant Nebridi 22, 08222 Terrassa, Catalonia, Spain.

Running title: Conformation of rhodopsin mutants in DHA phospholipid

[†] **Present address:** Group of Genetics in School of Bioscience and Technology, Weifang Medical University. Baotong West Street 7166, 261053 Weifang city, Shandong Province, China.

[‡] **Permanent address:** Campo Experimental Bajío (INIFAP). Km 6.5 Carretera Celaya-San Miguel Allende s/n. México. CP 38110.

[*]**Corresponding author:** Professor Pere Garriga, Grup de Biotecnologia Molecular i Industrial, Centre de Biotecnologia Molecular, Departament d'Enginyeria Química, Universitat Politècnica de Catalunya, Rambla de Sant Nebridi 22, 08222 Terrassa, Spain. Tel: +34 937398568; FAX: +34 937398225; E-mail: pere.garriga@upc.edu

ABSTRACT

Rhodopsin is the visual photoreceptor of the retinal rod cells that mediates dim light vision and a prototypical member of the G protein-coupled receptor superfamily. The structural stability and functional performance of rhodopsin are modulated by membrane lipids. Docosahexaenoic acid has been shown to interact with native rhodopsin but no direct evidence has been established on the effect of such lipid on the stability and regeneration of rhodopsin mutants associated with retinal diseases. The stability and regeneration of two thermosensitive mutants G90V and N55K, associated with the retinal degenerative disease retinitis pigmentosa, have been analyzed in docosohexaenoic phospholipid (1,2-didocosa-hexaenoyl-s*n*-glycero-3-phosphocholine; DDHA-PC) liposomes. G90V mutant reconstituted in DDHA-PC liposomes significantly increased its thermal stability, but N55K mutant showed similar thermal sensitivity both in dodecyl maltoside detergent solution and in DDHA-PC liposomes. The retinal release process, measured by fluorescence spectroscopy, became faster in the lipid system for the two mutants. The opsin conformation was stabilized for the G90V mutant allowing improved retinal uptake whereas no chromophore binding could be detected for N55K opsin after photoactivation. The results emphasize the distinct role of DHA on different phenotypic rhodopsin mutations associated with classical (G90V) and sector (N55K) retinitis pigmentosa.

Introduction

G protein-coupled receptors (GPCRs) constitute one of the largest protein families in the mammalian genome.[1] A wide range of different external stimuli are known to activate GPCRs, like ions, organic odorants, amines, peptides, proteins, lipids, nucleotides and photons enabling signal transduction to the interior of the cell.[2,3] Considering their roles in cell signal transduction, GPCRs are main targets for drug development towards a number of pathological conditions. GPCRs are grouped into six families with the rhodopsin (Rho)-like family (Class A) as the largest subfamily of receptors.[4] The visual photoreceptor Rho is a prototypical member for Class A GPCRs superfamily. Rho consists of a seven-helical transmembrane opsin apoprotein and an 11-*cis*-retinal chromophore, linked to K296 of the protein via a protonated Schiff Base (SB) linkage.[5,6] The atomic structure of the inactive dark state of Rho and other relevant conformational states have been determined by X-ray crystallography.[7,8] Upon photon absorption, 11-*cis*-retinal isomerizes to all-*trans*-retinal and triggers receptor activation by means of conformational rearrangements leading to the active metarhodopsin II (Meta II) conformation that initiates G-protein signal transduction.[6,9,10]

Retinitis pigmentosa (RP) is a diverse group of eye disorders causing retinal degeneration and leading to blindness.[11,12] RP associated with mutations in Rho is proposed as mainly a protein-misfolding disease caused by heterogeneous mutations which modify the cellular fate and induce photoreceptor cell death.[13–15] In addition to protein misfolding, other molecular mechanisms for RP, like retinal regeneration alterations and thermal instability have been proposed.[12,16,17] Typically, Rho mutants are purified in the mild neutral detergent *n*-Dodecyl-β-D-maltoside (DM) which may accentuate this structural instability.[18] To protect the membrane protein stability and function, a physiologically-relevant lipid bilayer environment was used.[19–22] Herein,

1,2-didocosa-hexaenoyl-*sn*-glycero-3-phosphocholine (DDHA-PC (22:6n-3)), formed by two DHA chains, was used to study the effect of this lipid on Rho mutant conformation and stability. DHA accounts for 50-60% of the total fatty acids in the retina and optimizes retinal integrity and visual function.[23–26] Compared with other phosphorylated lipids, such as saturated, long chain (14:0) DMPC, DMPG and DMPS,[27–29] DDHA-PC is unsaturated and highly specific to the retina and can modulate Rho stability and function.[22,24,30] We have previously demonstrated the specific role of DHA phspholipid in increasing native Rho thermal stability.[24] Therefore, the study of Rho mutants in DDHA-PC liposomes is a more appropriate system to reveal novel clues for understanding the degeneration mechanisms of RP in a native environment. To this aim, we have analyzed the conformational properties of the highly unstable G90V and N55K mutants associated with classical and sector RP, respectively.[31,32]

We have found that purified G90V and N55K mutants can be successfully reconstituted in DDHA-PC liposomes but the conformational properties of the two mutants are completely different. In the case of G90V, the lipid environment increased the thermal stability in the dark and improved opsin conformational stability allowing efficient ligand binding and chromophore regeneration after complete Meta II decay. DDHA-PC liposomes also speeded up the retinal release process. In the case of N55K, neither obvious thermal stability enhancement nor retinal entrance after Meta II decay in DDHA-PC liposomes were observed. The only feature that was shared with the G90V mutant was an accelerated retinal release rate after illumination. These results confirm the diverse effect of DDHA-PC on Rho mutants and highlight the different response of classical RP and sector RP mutants to the specific lipid environment depending on the conformational properties of these distinct mutations.

Experimental procedures

Materials

G90V and N55K opsin genes were cloned into the pMT4 plasmid. 11-*cis*-retinal chromophore was kindly provided from Dr. R. Crouch and the National Eye Institute, National Institutes of Health (USA). DDHA-PC (22:6n-3) was purchased from Avanti Polar Lipids Inc (Alabaster, AL). DM was from Anatrace (Maumee, OH, USA). Chloroform was purchased from Sigma-Aldrich (Sant Louis, MO), methanol was from Panreac (Barcelona, Spain) and the polystyrene beads (Bio-beads SM-2) used for DM removal were provided by Bio-Rad Laboratories, Inc. (Hercules, CA). Polyethyleneimine 25 kDa (PEI) was purchased from Polysciences (Warrington, PA, USA). Purified mAb rho-1D4 was purchased from Cell Essentials (Boston, MA USA) and coupled to CNBr-activated Sepharose 4B Fast Flow (Amersham Biosciences). The 1D4 9-mer peptide H-TETSQVAPA-OH was synthesized by Unitat de Tecniques Separatives i Sintesi de Peptids (Universitat de Barcelona, Spain). Hydroxylamine, protease inhibitor cocktail and phenylmethanesulfonyl (PMSF) were from Sigma-Aldrich (St. Louis, MO, USA).

Buffers

The following buffers were used: PBS: 137 mM NaCl, 2.7 mM KCl, 1.5 mM KH_2PO_4, and 8 mM Na_2HPO_4, pH 7.4; washing buffer: PBS containing 0.05% DM.

Cell culture materials

COS-1 cells were purchased from the American Type Culture Collection (Manassas, VA, USA), DMEM, fetal bovine serum, L-glutamine and antibiotics penicillin-streptomycin were from Sigma-Aldrich (St. Louis, MO, USA), OPTIMEM

reduced Serum Media for DNA transfection was from Life Technologies (Madrid, Spain).

Methods

Expression and purification of Rho WT and G90V, N55K mutants

Bovine recombinant wild type (WT) Rho, and the G90V and N55K mutants genes were constructed in the pMT4 plasmid vectors by site-directed mutagenesis.[33] Plasmids were transfected into five COS-1 cell plates, at 85% confluence, by using PEI with 30 µg of plasmid DNA per 145 cm plate. After 48 h, cells were harvested and regenerated with 10 µM 11-*cis*-retinal in PBS by overnight incubation. Cells solubilization was carried out by 1 h incubation with 1% (w/v) DM, 100 µM PMSF and protease inhibitors at 4ºC, followed by ultracentrifugation at 30,000 rpm for 30 min (in a Ti50 rotor). The supernatants obtained were used for immunoaffinity chromatography purification by means of Rho-1D4 antibody coupled to sepharose beads to a final concentration of 52.5 µg/ml. After 3 h incubation, the Rho-1D4-sepharose-bound WT or mutants were eluted with PBS containing 0.05% DM and 100 µM 1D4 9-mer peptide.[18] The protein was immediately used or stored at -80°C.

Preparation of DDHA-PC proteoliposomes

DDHA-PC powder was dissolved in chloroform: methanol (2:1, v/v) and the solution was evaporated to dryness under a stream of nitrogen until no solvent trace was detected. The lipid film was hydrated with PBS pH 7.4 to obtain the liposomes. The liposomes were mixed with 0.5% DM and the solubilized protein was subject to gentle agitation for 30 min at 4°C. Bio-beads SM-2 were added to extract the extra DM.[34] Finally, the

proteoliposomes system consisted of 1.05 mM DDHA-PC liposomes and 1.4 µM WT or mutants (750:1 molar ratio).

Ultraviolet-visible (UV-Vis) absorption spectra of WT, G90V and N55K

All the measurements were carried out in a Cary 100Bio spectrophotometer (Varian, Australia), equipped with water-jacketed cuvette holders connected to a circulating water bath. A Peltier accessory connected to the spectrophotometer was used to control the temperature. All spectra were recorded in the 250 nm-650 nm range with a bandwidth of 2 mm, a response time of 0.1 s, and a scan speed of 300 nm/min.

Thermal bleaching assay by UV-Vis spectroscopy

UV-Vis spectroscopy was used to follow WT and mutants thermal stability. WT and mutants thermal bleaching rates were obtained, in the dark, by monitoring the decrease of the maximum absorbance value in the visible spectral band (λ_{max}) over time at 48°C. Spectra were recorded every min. Data points were obtained by using the equation $\Delta A = (A - A_f)/(A_0 - A_f)$, where A is the absorbance at λ_{max}, A_f is the absorbance at the final time, and A_0 is the absorbance at time 0. The half-life time ($t_{1/2}$) for the process was determined by fitting the experimental data to single exponential decay curves using Sigma Plot version 11.0 (Systat Software, Chicago, IL, USA). Experiments were performed at least three times using independently purified samples.

Retinal release kinetics and opsin conformational stability by fluorescence spectroscopy

Fluorescence spectroscopic measurements were carried out with a Photon Technologies QM-1 steady-state fluorescence spectrophotometer (PTI Technologies, Birmingham, NJ, USA). The sample temperature was controlled with a cuvette holder Peltier

accessory TLC 50 (Quantum Northwest, Liberty Lake, WA, USA) connected to a hybrid liquid coolant system Reserator XT (Zalman, Garden Grove, CA, USA).

Upon illumination, the chromophore undergoes isomerization from 11-*cis* to all-*trans* configuration with subsequent formation of the active Meta II conformation. Under our experimental conditions, the Meta II decay parallels the retinal release process. Thus, Meta II decay is followed by the Trp fluorescence increase at 330 nm due to the retinal release from the opsin apoprotein. Fluorescence was monitored over time with an excitation wavelength of 295 nm and an emission wavelength of 330 nm. All fluorescence spectra were carried out by exciting the samples for 2 s at $\lambda_{295\,nm}$ and a slit bandwidth of 0.5 nm and blocking the excitation beam for 28 s with a beam shutter to avoid photobleaching of the sample. Trp emission was monitored at $\lambda_{330\,nm}$ with a slit bandwidth of 10 nm.

WT or mutants dissolved in PBS containing 0.05% DM or in PBS containing DDHA-PC liposomes were kept at 20°C for 10 min to stabilize the fluorescence emission, followed by 30 s illumination with a 150-watt power source equipped with a cut-off filter (λ> 495 nm) to form Meta II. The fluorescence curve increased until it reached a plateau (Meta II completely decayed to opsin and free all-*trans*-retinal), and then fresh 11-*cis*-retinal was added and the fluorescence signal was quenched due to retinal uptake by opsin. Experiments were performed at least three times using independently purified samples.

Results

UV-Vis spectrophotometry of purified WT and mutants

The UV-Vis spectral features of WT, G90V and N55K mutants in detergent DM solution are very similar to those previously reported (Figure 1).[31,32] For all opsins, the dark-state

spectra showed two main characteristic bands: one at λ_{280nm} corresponding to the opsin apoprotein and the other at the visible region corresponding to the retinal chromophore covalently bound to the protein.[35] The λ_{max} value of the visible chromophoric band of WT, G90V and N55K mutant is 499 nm, 489 nm and 495 nm respectively. In DM detergent, the A_{280}/A_{max} ratio of WT is 1.9, whereas the ratio of G90V and N55K is 3.5 and 6.3, respectively, being much higher than WT (Figure 1). This higher A_{280}/A_{max} ratio could be associated with possible misfolding, aggregation or regeneration impairment of the mutants.

UV-Vis spectroscopy was also used to characterize Rho behavior after illumination. Upon 30 s illumination, photoactived WT showed the typical shift of the visible absorbance band towards 380 nm (Figure 1) in DM. On the other hand, G90V and N55K showed an incomplete conversion of the visible band in DM,[31] compatible with the formation of a photointermediate containing a protonated SB linkage.[32] The photobleaching behaviour is better appreciated in the difference spectra (insets in Figure 1).

The WT and mutants spectra were also recorded in DDHA-PC liposomes (Figure 2). WT, G90V and N55K mutants were purified from COS-1 cells by transient transfection and inserted into DDHA-PC liposomes as described above (see Materials and Methods). In all cases, the λ_{max} values in DDHA-PC liposomes are the same as those in DM detergent.[31] With the presence of DDHA-PC liposomes, the ratio A_{280}/A_{max} of WT and mutants increased largely compared to DM conditions. The higher A_{280}/A_{max} ratio in liposomes is mainly caused by the liposomes background absorption rather than an increase in protein misfolding or aggregation as observed in control spectra of DDHA-PC liposomes alone (data not shown). The photobleaching behaviour observed is similar to that in DM solution (Figure 2, insets). Additional electrophoretic analysis appeared to indicate

changes in the oligomeric status of rhodopsin in DDHA-PC liposomes (Figure 1, supplementary information).

DDHA-PC liposomes increase WT and G90V thermal stability

The thermal stability of the dark state conformations of WT and G90V and N55K mutants in DM and in DDHA-PC were measured at 48ºC.[31] The thermal decay process in the dark is associated with retinal chromophore isomerization, hydrolysis of the protonated SB linkage, and eventual protein irreversible denaturation.[36,37] The stabilizing effect of DDHA-PC lipids on WT can be clearly observed (Table 1 and Figure 3) (WT_{DM} $t_{1/2}$ = 21±5, R^2= 0.9812 and $WT_{liposomes}$ $t_{1/2}$>500, R^2= 0.7146) and is similar to previously results observed in native bovine rhodopsin.[24] $G90V_{liposomes}$ thermal stability was higher ($t_{1/2}$ = 2.8±0.2 min; R^2= 0.9527) compared to $G90V_{DM}$ ($t_{1/2}$ = 0.7±0.1 min, R^2= 0.9902) indicating that the mutant structure was protected by the DDHA-PC liposomes bilayer.[37] In contrast, $N55K_{liposomes}$ ($t_{1/2,}$= 1.8±0.1 min, R^2= 0.9479) did not show a significant increase compared to $N55K_{DM}$ ($t_{1/2}$ =1.6±0.1 min, R^2= 0.9612) (Table 1 and Figure 3). The main finding is that DDHA-PC could significantly stabilize the dark conformation of WT and G90V mutant, whereas no significant increase in stability could be detected for the N55K mutant (Figure 3). This marked effect appears to be specific of the DDHA-PC system because experiments conducted with DMPC liposomes do not provide the same degree of stabilization (Figure 2, supplementary information).

Retinal release kinetics and opsin conformational stability

WT_{DM} or $WT_{liposomes}$, were kept in the fluorescence cuvette in the dark until Trp fluorescence showed a flat stable baseline. Upon illumination, Trp fluorescence signal started to increase, due to the retinal release from the Meta II conformation. After complete Meta II decay (the fluorescence curve reached a plateau), exogenous

11-*cis*-retinal was added (in a 2.5:1, retinal: opsin molar ratio) to test whether the added retinal could re-enter the binding pocket or not. WT_{DM} showed no significant decrease in the fluorescence signal upon retinal addition after Meta II complete decay (Figure 4) indicating that the retinal could not enter to the opsin binding pocket. In contrast, $WT_{liposomes}$ showed an obvious decrease of fluorescence signal suggesting chromophore re-entry to the binding pocket thus quenching the Trp fluorescence. After Meta II completely decay, both $G90V_{DM}$ and $G90V_{liposomes}$ exhibited a fluorescence signal decrease indicating retinal entrance into the pocket. The sector RP mutant N55K displayed a completely different response.[32] Addition of exogenous retinal did not cause any fluorescence signal change, meaning that retinal did not enter the retinal binding pocket either in $N55K_{DM}$ or in $N55K_{liposomes}$ (Figure 4).

The $t_{1/2}$ of retinal release for WT, G90V and N55K mutants in DM or DDHA-PC liposomes were determined (Table 1 and Figure 4). In DDHA-PC liposomes environment, WT, G90V and N55K presented a faster retinal release process than in DM detergent. The $t_{1/2}$ of the retinal release process decreased from 14.3 min in DM to 4.4 min in liposomes for WT, from 23.4 min in DM to 15.3 min for $G90V_{liposomes}$, and from 9.5 min in DM to 4.7 min in liposomes for N55K.

Discussion

DHA is present at high concentrations in the retina and in the brain. The functional role of this molecules has been previously investigated in the past decades.[26,38–40] As the major polyunsaturated fatty acid in the rod outer segments of the photoreceptor cells, DHA level was associated with altered photoreceptor function in n-3 fatty acids deficient animals.[38,41] It was also proposed that efficient and rapid propagation of G protein-coupled signaling is optimized by DHA phospholipid acyl chains.[42] In a previous

study, we demonstrated the specificity of DHA in stabilizing native Rho as compared with other phospholipids that did not produce any stability increase.[24] In our current study we used DDHA-PC to obtain liposomes to investigate the effect of this system on the stability and regeneration properties of Rho mutants associated with RP for the first time. Our main aim was to try to revert some of the conformational features (namely conformational instability) caused by mutations in Rho associated with the retinal degenerative RP disease. G90V located in helix 2, associated with classical RP, and N55K located in helix 1, associated with sector RP were used as prototypic mutations in order to study with the potential effect of DHA *in vitro.*

UV-Vis spectroscopy was used to monitor the chromophore changes in WT, and G90V and N55K mutants upon photobleaching, and compared between DM and DDHA-PC liposomes conditions (Figures 1 and 2). After 30 s illumination, WT $_{liposomes}$ displayed a complete conversion of the visible band to the 380 nm absorbing species; the same behavior observed in DM detergent. In contrast, the mutants, but particularly $N55K_{liposomes}$, showed a slight partial photoconversion of the visible species to a photointermediate with a protonated SB linkage, when compared to DM conditions.

We have found that DDHA-PC liposomes improve the thermal stability of Rho compared with DM solution. When reconstituted into DDHA-PC liposomes (Figure 3), $G90V_{liposomes}$ increased 4-fold the thermal stability compared to $G90V_{DM}$ at 48ºC suggesting that the SB linkage was better protected from hydrolysis.[37] Contrarily, N55K showed similar thermal stability both in DM and in DDHA-PC liposomes. This finding shows that the lipid environment does not improve the stability of the N55K mutant as in the case of G90V, suggesting a strong disruptive effect of the mutation for the sector RP N55K mutation.

DDHA-PC liposomes accelerate the 11-*cis*-retinal release rate according to the fluorescence spectroscopic experiments (Figure 4). $T_{1/2}$ for the retinal release process of WT G90V, and N55K in liposomes is faster in all cases than in DM detergent. After Meta II decay, the addition of exogenous 11-*cis*-retinal did not result in retinal uptake by WT_{DM}, but allowed retinal binding to opsin in $WT_{liposomes}$. $G90V_{DM}$ opsin showed partial ability to bind the 11-*cis*-retinal chromophore, and this ability was enhanced in $G90V_{liposomes}$ meaning that the lipid environment facilitated the retinal uptake for this mutant. G90V, when compared to WT, showed a distinctive behavior, suggesting a more flexible and open opsin conformation already in DM whose conformational features could be enhanced in liposomes. Interestingly, N55K did not show any fluorescence decrease either in liposomes or in DM (Table 1 and Figure 4). This particular phenotype can be associated with a specific role of the introduced lysine,[32] at the cytoplasmic side of TMs 1, 2 and 7 close to this residue, that could affect retinal accessibility/release to/from the opsin binding pocket. In addition the reduced stability of the dark-state conformation of the receptor would also certainly contribute to the observed fluorescence results. This residue is located nearby the prospective retinal channel proposed in Rho.[43] The unperturbed fluorescence spectra, upon retinal addition to N55K, suggest a lack of retinal binding to the N55K opsin pocket (Figure 4). This could lead to impaired receptor recycling causing protein aggregation and subsequent degradation. A plausible hypothesis is that the N55K degradation pathway would become overloaded with non-regenerated and aggregated N55K that would be toxic to the retinal cells being responsible for the sector clinical phenotype. In this regards, the particular phenotype of N55K has been associated with sector RP and the potential effect of light.[32]

The neutral polyunsaturated DHA chains can play a key biological function in lipid-protein interactions associated with the complex process of vision. We have shown

that DHA increases the thermal stability of the G90V mutant but not significantly that of the N55K mutant, which could be consistent with the lipid-protein region of interaction and its specific physiological response. DHA does not appear to protect the opsin conformation in the case of the N55K mutant, as in the case of the classical RP G90V mutant and it does not facilitate retinal uptake after complete MetaII decay. This effect could be associated with the specific role of the lysine mutation as discussed previously.[32] The results obtained emphasize the distinct role of DHA on the G90V and N55K mutations associated with different RP phenotypes.

The effects observed can be associated with the chemical nature of the DHA lipid. Different from saturated and monounsaturated hydrocarbon chains, the neutral polyunsaturated DHA has a unique chemical structure with six cis-locked double bounds. The number of freedom degrees of DHA chains is substantially lower which could be indicative of rigidity. Polyunsaturated chains in crystals form highly ordered, elongated structures with angle-iron or helical arrangement of double bonds. The experimental results suggest that the low order in bilayers with high DHA content is a direct consequence of both high conformational flexibility and rapid structural conversions of DHA chains themselves without significant energetic penalty.[44] NMR data proved that the photointermediate Meta III had stronger contact with DHA compared with dark Rho, Meta I and Meta II states. DHA enrichment may enhance protein function both by a change of general membrane properties as well as by specific interactions with particular regions of the protein.[44] N55K, located in helix 1, and G90V located in helix 2, are structurally located near residues 48, 50, 92, 95, 96 which are tightly packed with DHA in a molecular model.[45] This specific location of the mutation sites in the Rho three-dimensional structure could justify the observed effects of DHA liposomes on the

mutants behaviour in the thermal stability and chromophore binding after photoactivation.

Acknowledgements

This work was supported by the grant Ministerio de Ciencia e Innovación (Spain) (SAF2011-30216-C02-01). Grups de Recerca Consolidats from Generalitat de Catalunya (2009 SGR 1402), and a grant from Fundación Areces to PG. XD is the recipient of pre-doctoral scholarship from the Chinese Scholarship Council (CSC).

Abbreviations

WT, wild type rhodopsin; DM, *n*-Dodecyl-D-maltoside; DHA, docosahexaenoic acid; DDHA-PC, 1,2-didocosa-hexaenoyl-*sn*-glycero-3-phosphocholine; DMPC, 1,2-dimyristoyl-*sn*-glycero-3-phosphatidylcholine; DMPG, 1,2-dimyristoyl-*sn*-glycero-3-phospho-(1′-rac-glycerol); DMPS, 1,2-dimyristoyl-*sn*-glycero-3-phospho-L-serine; GPCRs, G-protein-coupled receptors; λ_{max}, lambda max; Meta II, Metarhodopsin II; Rho, rhodopsin; RP, retinitis pigmentosa; $t_{1/2}$, half-life time; SB, Schiff Base;

References

1. Lander, E. S. *et al.* Initial sequencing and analysis of the human genome. *Nature* **409,** 860–921 (2001).

2. Fredriksson, R., Lagerstrom, M. C., Lundin, L.-G. & Schioth, H. B. The G-protein-coupled receptors in the human genome form five main families. Phylogenetic analysis, paralogon groups, and fingerprints. *Mol. Pharmacol.* **63,** 1256–1272 (2003).

3. Sarramegna, V., Talmont, F., Demange, P. & Milon, a. Heterologous expression of G-protein-coupled receptors: Comparison of expression systems from the standpoint of large-scale production and purification. *Cell. Mol. Life Sci.* **60,** 1529–1546 (2003).

4. Gao, Q.-B. & Wang, Z.-Z. Classification of G-protein coupled receptors at four levels. *Protein Eng. Des. Sel.* **19,** 511–516 (2006).

5. Wang, T. & Duan, Y. Retinal release from opsin in molecular dynamics simulations. *J. Mol. Recognit.* **24,** 350–8 (2011).

6. Menon, S. T., Han, M. & Sakmar, T. P. Rhodopsin: structural basis of molecular physiology. *Physiol. Rev.* **81,** 1659–1688 (2001).

7. Hofmann, K. P. *et al.* A G protein-coupled receptor at work: the rhodopsin model. *Trends Biochem. Sci.* **34,** 540–52 (2009).

8. Choe, H.-W. *et al.* Crystal structure of metarhodopsin II. *Nature* **471,** 651–655 (2011).

9. Lamb, T. D. & Pugh, E. N. Phototransduction, dark adaptation, and rhodopsin regeneration the proctor lecture. *Invest. Ophthalmol. Vis. Sci.* **47,** 5137–52 (2006).

10. Yau, K.-W. & Hardie, R. C. Phototransduction motifs and variations. *Cell* **139,** 246–264 (2009).

11. Hernandez-Rodriguez, E. W. *et al.* Understanding rhodopsin mutations linked to the retinitis pigmentosa disease: a QM/MM and DFT/MRCI study. *J. Phys. Chem. B* **116,** 1060–1076 (2012).

12. Krebs, M. P. *et al.* Molecular mechanisms of rhodopsin retinitis pigmentosa and the efficacy of pharmacological rescue. *J. Mol. Biol.* **395,** 1063–1078 (2010).

13. Tzekov, R., Stein, L. & Kaushal, S. Protein misfolding and retinal degeneration. *Cold Spring Harb. Perspect. Biol.* **3,** a007492 (2011).

14. Gregersen, N., Bross, P., Vang, S. & Christensen, J. H. Protein misfolding and human disease. *Annu. Rev. Genomics Hum. Genet.* **7,** 103–124 (2006).

15. Petrs-Silva, H. & Linden, R. Advances in gene therapy technologies to treat retinitis pigmentosa. *Clin. Ophthalmol.* **8,** 127–136 (2014).

16. Saliba, R. S., Munro, P. M. G., Luthert, P. J. & Cheetham, M. E. The cellular fate of mutant rhodopsin: quality control , degradation and aggresome formation. (2002).

17. Andrés, A., Garriga, P. & Manyosa, J. Altered functionality in rhodopsin point mutants associated with retinitis pigmentosa. *Biochem. Biophys. Res. Commun.* **303,** 294–301 (2003).

18. Ramon, E. *et al.* Effect of dodecyl maltoside detergent on rhodopsin stability and function. *Vision Res.* **43,** 3055–3061 (2003).

19. Cho, H. S., Dominick, J. L. & Spence, M. M. Lipid domains in bicelles containing unsaturated lipids and cholesterol. *J. Phys. Chem. B* **114,** 9238–9245 (2010).

20. Marsh, D. Protein modulation of lipids, and vice-versa, in membranes. *Biochim. Biophys. Acta - Biomembr.* **1778,** 1545–1575 (2008).

21. Soubias, O., Niu, S. L., Mitchell, D. C. & Gawrisc, K. Lipid-rhodopsin hydrophobic mismatch alters rhodopsin helical content. *J. Am. Chem. Soc.* **130,** 12465–12471 (2008).

22. Niu, L., Kim, J.-M. & Khorana, H. G. Structure and function in rhodopsin: asymmetric reconstitution of rhodopsin in liposomes. *Proc. Natl. Acad. Sci. U. S. A.* **99,** 13409–12 (2002).

23. Mitchell, D. C., Niu, S. L. & Litman, B. J. Enhancement of G protein-coupled signaling by DHA phospholipids. *Lipids* **38,** 437–443 (2003).

24. Sanchez-Martin, M. J., Ramon, E., Torrent-Burgues, J. & Garriga, P. Improved conformational stability of the visual G protein-coupled receptor rhodopsin by specific interaction with docosahexaenoic acid phospholipid. *Chembiochem* **14,** 639–644 (2013).

25. Oates, J. & Watts, A. Uncovering the intimate relationship between lipids, cholesterol and GPCR activation. *Curr. Opin. Struct. Biol.* **21,** 802–807 (2011).

26. Anderson, G. J., Connor, W. E. & Corliss, J. D. Docosahexaenoic acid is the preferred dietary n-3 fatty acid for the development of the brain and retina. *Pediatr. Res.* **27,** 89–97 (1990).

27. Ujwal, R. & Bowie, J. U. Crystallizing membrane proteins using lipidic bicelles. *Methods* **55,** 337–341 (2011).

28. Kaya, A. I., Thaker, T. M., Preininger, A. M., Iverson, T. M. & Hamm, H. E. Coupling efficiency of rhodopsin and transducin in bicelles. *Biochemistry* **50,** 3193–3203 (2011).

29. McKibbin, C. *et al.* Opsin stability and folding: modulation by phospholipid bicelles. *J. Mol. Biol.* **374,** 1319–1332 (2007).

30. Serebryany, E., Zhu, G. A. & Yan, E. C. Y. Artificial membrane-like environments for in vitro studies of purified G-protein coupled receptors. *Biochim. Biophys. Acta* **1818,** 225–233 (2012).

31. Toledo, D. *et al.* Molecular mechanisms of disease for mutations at Gly-90 in rhodopsin. *J. Biol. Chem.* **286,** 39993–40001 (2011).

32. Ramon, E. *et al.* Differential light-induced responses in sectorial inherited retinal degeneration. *J. Biol. Chem.* **289,** 35918–35928 (2014).

33. Oprian, D. D., Molday, R. S., Kaufman, R. J. & Khorana, H. G. Expression of a synthetic bovine rhodopsin gene in monkey kidney cells. *Proc. Natl. Acad. Sci. U. S. A.* **84,** 8874–8878 (1987).

34. Merino, S., Domenech, O., Vinas, M., Montero, M. T. & Hernandez-Borrell, J. Effects of lactose permease on the phospholipid environment in which it is

reconstituted: a fluorescence and atomic force microscopy study. *Langmuir* **21,** 4642–4647 (2005).

35. Reeves, P. J., Hwa, J. & Khorana, H. G. Structure and function in rhodopsin: kinetic studies of retinal binding to purified opsin mutants in defined phospholipid-detergent mixtures serve as probes of the retinal binding pocket. *Proc. Natl. Acad. Sci. U. S. A.* **96,** 1927–1931 (1999).

36. Landin, J. S., Katragadda, M. & Albert, a. D. Thermal destabilization of rhodopsin and opsin by proteolytic cleavage in bovine rod outer segment disk membranes. *Biochemistry* **40,** 11176–11183 (2001).

37. Liu, J. *et al.* Thermal Decay of Rhodopsin : Role of Hydrogen Bonds in Thermal Isomerization of 11- cis Retinal in the Binding Site and Hydrolysis of Protonated Schiff Base. **19,** 8750–8751 (2009).

38. Jastrzebska, B., Debinski, A., Filipek, S. & Palczewski, K. Role of membrane integrity on G protein-coupled receptors: Rhodopsin stability and function. *Prog. Lipid Res.* **50,** 267–77 (2011).

39. Daemen, F. J. Vertebrate rod outer segment membranes. *Biochim. Biophys. Acta* **300,** 255–288 (1973).

40. Fliesler, S. J. & Anderson, R. E. Chemistry and metabolism of lipids in the vertebrate retina. *Prog. Lipid Res.* **22,** 79–131 (1983).

41. Jeffrey, B. G., Mitchell, D. C., Gibson, R. a. & Neuringer, M. N-3 Fatty Acid Deficiency Alters Recovery of the Rod Photoresponse in Rhesus Monkeys. *Investig. Ophthalmol. Vis. Sci.* **43,** 2806–2814 (2002).

42. Fischer, T. H. & Williams, T. P. The effect of phospholipid structure on the thermal stability of rhodopsin. *Biochim. Biophys. Acta* **707,** 273–279 (1982).

43. Hildebrand, P. W. *et al.* A ligand channel through the G protein coupled receptor opsin. *PLoS One* **4,** e4382 (2009).

44. Gawrisch, K., Soubias, O. & Mihailescu, M. Insights from biophysical studies on the role of polyunsaturated fatty acids for function of G-protein coupled membrane receptors. *Prostaglandins. Leukot. Essent. Fatty Acids* **79,** 131–134 (2008).

45. Grossfield, A., Feller, S. E. & Pitman, M. C. A role for direct interactions in the modulation of rhodopsin by omega 3 polyunsaturated lipids. *Natl. Acad. Sci.* **103,** 4888–4893 (2006).

Table 1. Thermal Stability and Kinetics for the retinal release from the binding pocket of WT, and G90V and N55K mutants in PBS containing 0.05% DM or DDHA-PC liposomes. $t_{1/2}$ (in minutes) for the thermal decay was obtained by monitoring the decrease of A_{max} when samples were incubated at 48ºC in PBS and DM or DDHA-PC liposomes. The $t_{1/2}$ of retinal release was determined from the fluorescence curves. The $t_{1/2}$ of retinal release clearly decreased in DDHA-PC liposomes in all cases. The $t_{1/2}$ for the processes were determined by fitting the experimental data to single exponential decay curves using Sigma Plot version 11.0. All average and standard deviation were determined from three independent experiments. Statistical significance was determined by unpaired two-tailed Student's t-test using SigmaPlot. P values < 0.05 were considered to be statistically significant. In our study, the differences found between DM and DDHA-PC were statistically significant except in the case of N55K(*) mutant thermal decay.

	Thermal Decay (min)		Retinal release (min)	
	DM	DDHA-PC liposomes	DM	DDHA-PC liposomes
WT	21±5	>500	14.3 ± 0.9	4.4 ± 0.4
G90V	0.7±0.1	2.8±0.2	23.4 ± 0.3	15.3 ± 0.3
N55K	1.6±0.1*	1.8±0.1*	9.5 ± 0.4	4.7 ± 0.3

Figure legends

Figure 1. UV-Vis characterization of purified WT, N55K and G90V regenerated with 11-*cis*-retinal in DM. WT, and G90V and N55K mutants were expressed in COS-1 cells and immunopurified in PBS buffer with 0.05% DM. Spectra were recorded at 20ºC. Illumination was carried out for 30 s with a 150 W power source equipped with an optic fiber guide using a $\lambda > 495$ nm cut-off filter. (—) Dark state. (····) photobleached state; insets, difference spectra (dark minus light). The spectra are representative of three independent measurements.

Figure 2. UV-Vis characterization of purified WT, N55K and G90V regenerated with 11-*cis*-retinal in DDHA-PC liposomes. WT, and G90V and N55K mutants were purified and reconstituted into DDHA-PC liposomes. Spectra were recorded at 20ºC. Illumination was carried out for 30 s with a 150 W power source equipped with an optic fiber guide using a $\lambda > 495$ nm cut-off filter. (—) Dark state. (····) photobleached state; insets, difference spectra (dark minus light). The spectra are representative of three independent measurements.

Figure 3. Thermal stability of WT, G90V and N55K mutants in PBS containing DM (•) or liposomes (o) at 48°C. WT (upper panel), G90V (middle panel) and N55K (lower panel) mutants were purified from COS-1 cells and dissolved in PBS containing DM (•) or DDHA-PC liposomes (o). The samples were treated at 48ºC and the spectroscopic changes measured by means of UV-Vis spectrophotometry. All the data were recorded in the dark. Curves were fit to an exponential decay function. The insert of G90V and N55K shows the thermal decay during the first 5 minutes. WT and G90V mutant in DDHA-PC liposomes increases 4.2 times its thermal stability compared to the mutant in 0.05% DM. N55K mutant did not show any thermal decay improvement when comparing DM and

DDHA-PC liposomes conditions. The spectra represent the average and standard deviation of three independent measurements.

Figure 4. Fluorescence spectroscopy to monitor Meta II decay and retinal uptake kinetics for WT and G90V, N55K mutant in PBS containing (A) DM or (B) DDHA-PC liposomes. Fluorescence intensity of purified WT and mutants Rho were stabilized at 20°C in the dark and illuminated for 30 s. Upon MetaII decay and fluorescence stabilization, exogenous 11-*cis*-retinal was added. All fluorescence spectra were carried out by exciting the samples for 2 s at 295 nm and a slit bandwidth of 0.5 nm. 11-*cis*-retinal re-enters the binding pocket in $WT_{liposomes}$ but not in WT_{DM}. G90V can uptake the exogenous 11-*cis*-retinal both in DM and in DDHA-PC liposomes conditions. Interestingly, $G90V_{liposomes}$ shows more 11-*cis*-retinal entry capacity. On the other hand, the sectorial RP mutant, N55K, remains unaltered in both conditions. The spectra are representative of three independent measurements.

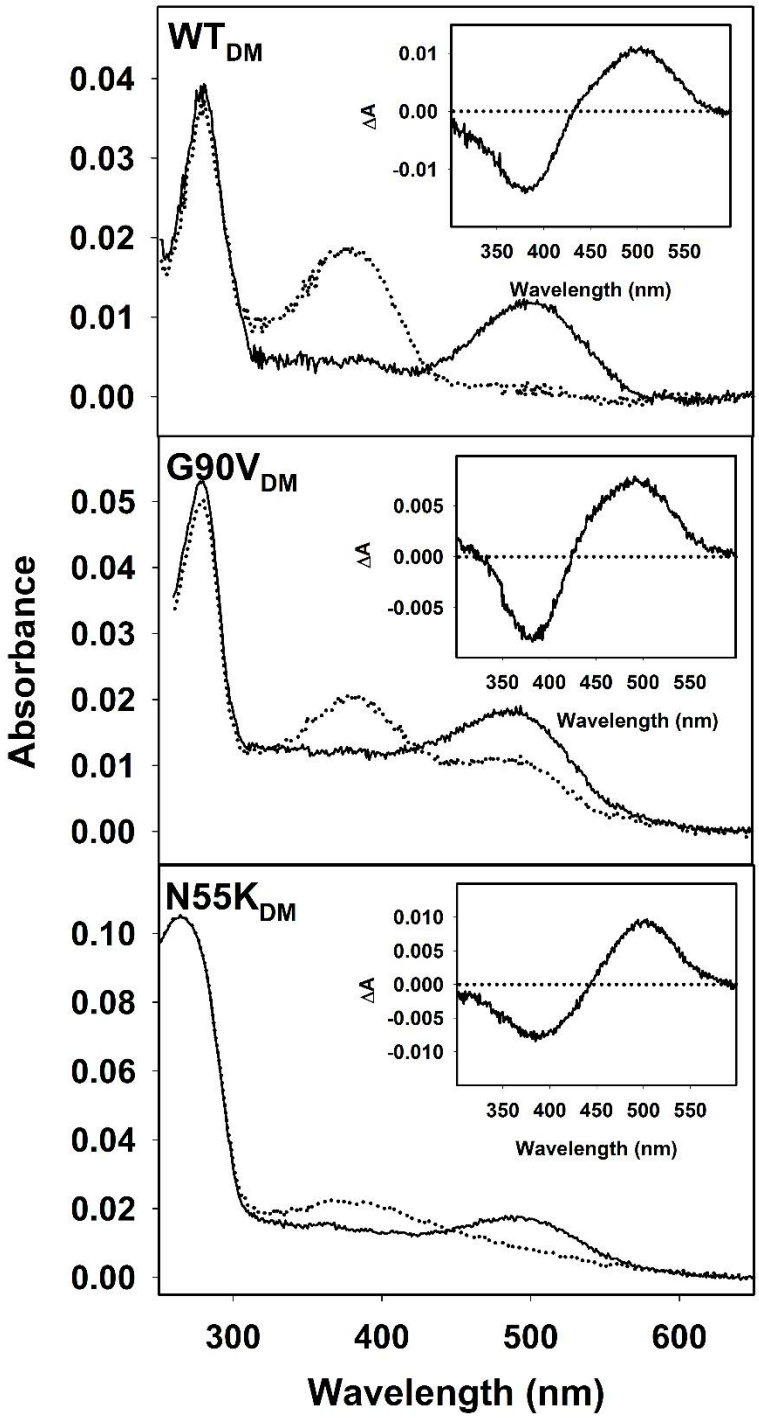

Figure 1

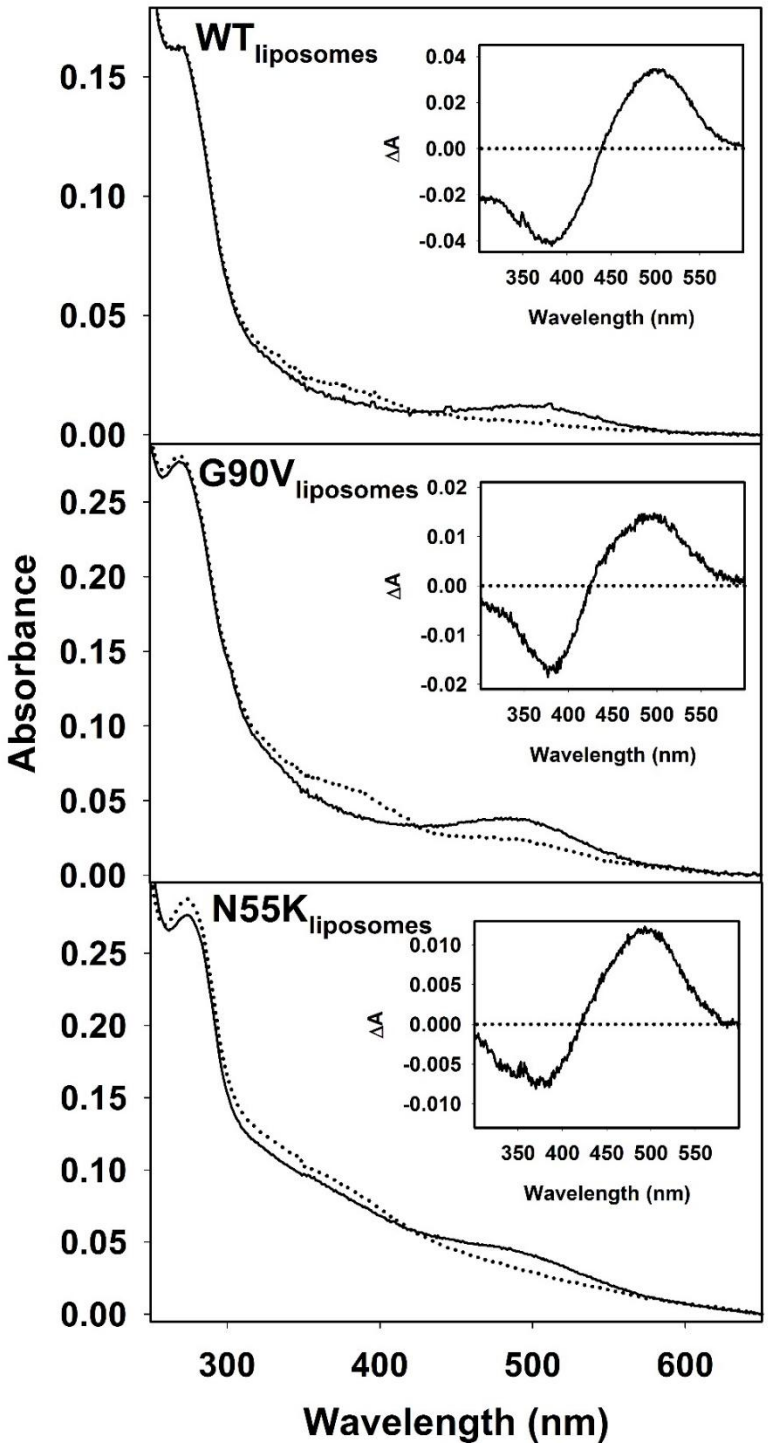

Figure 2

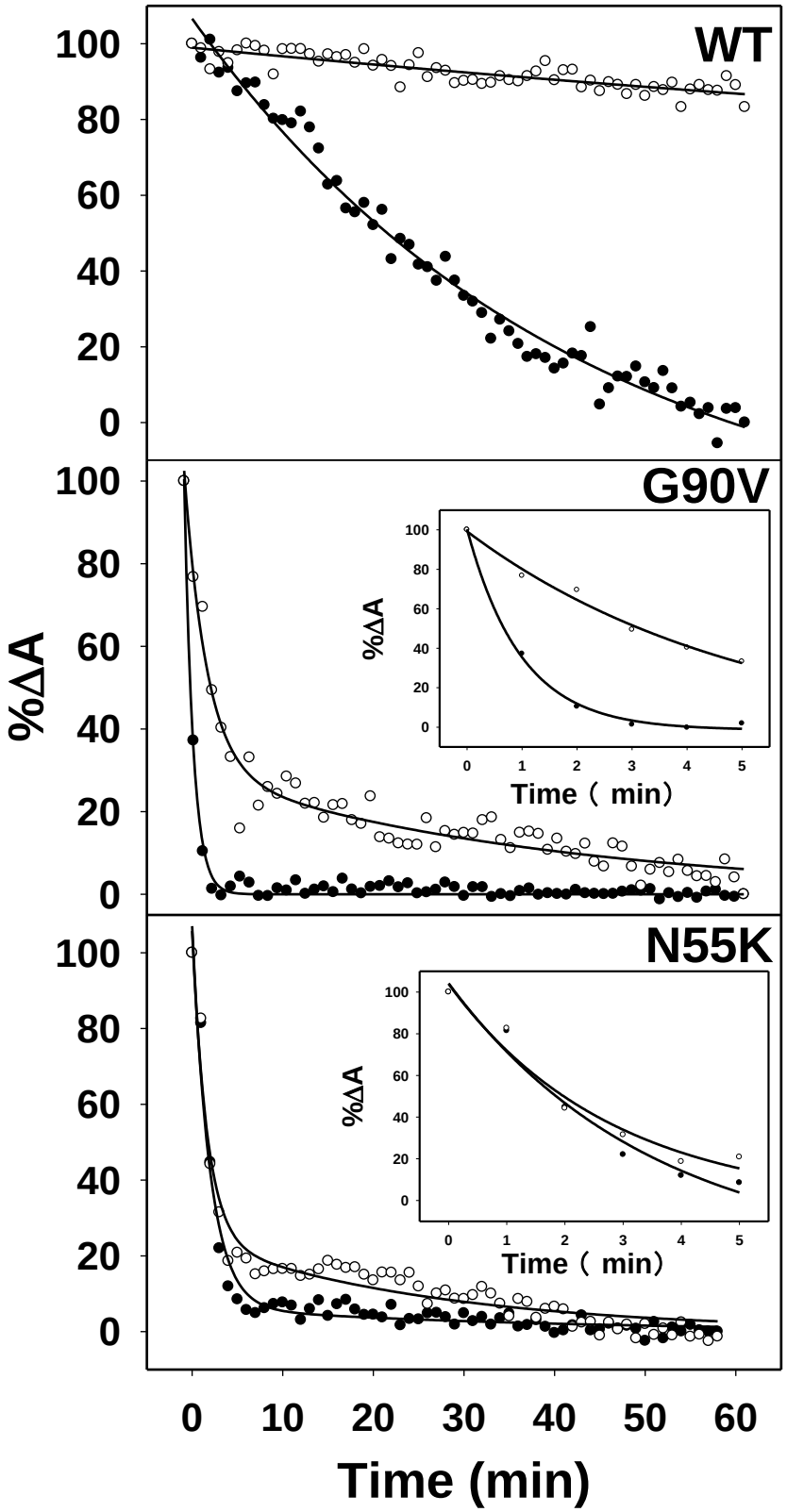

Figure 3

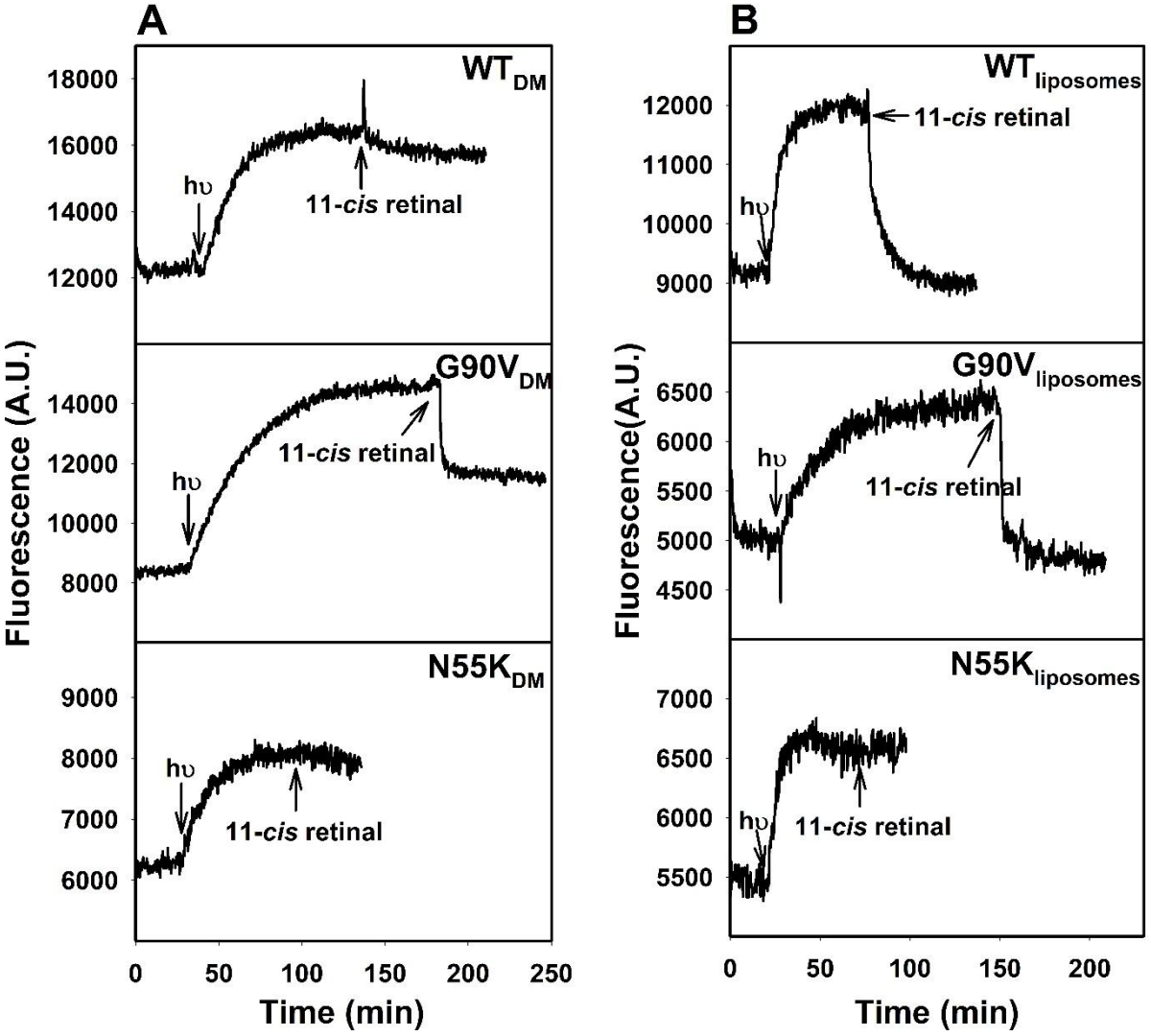

Figure 4

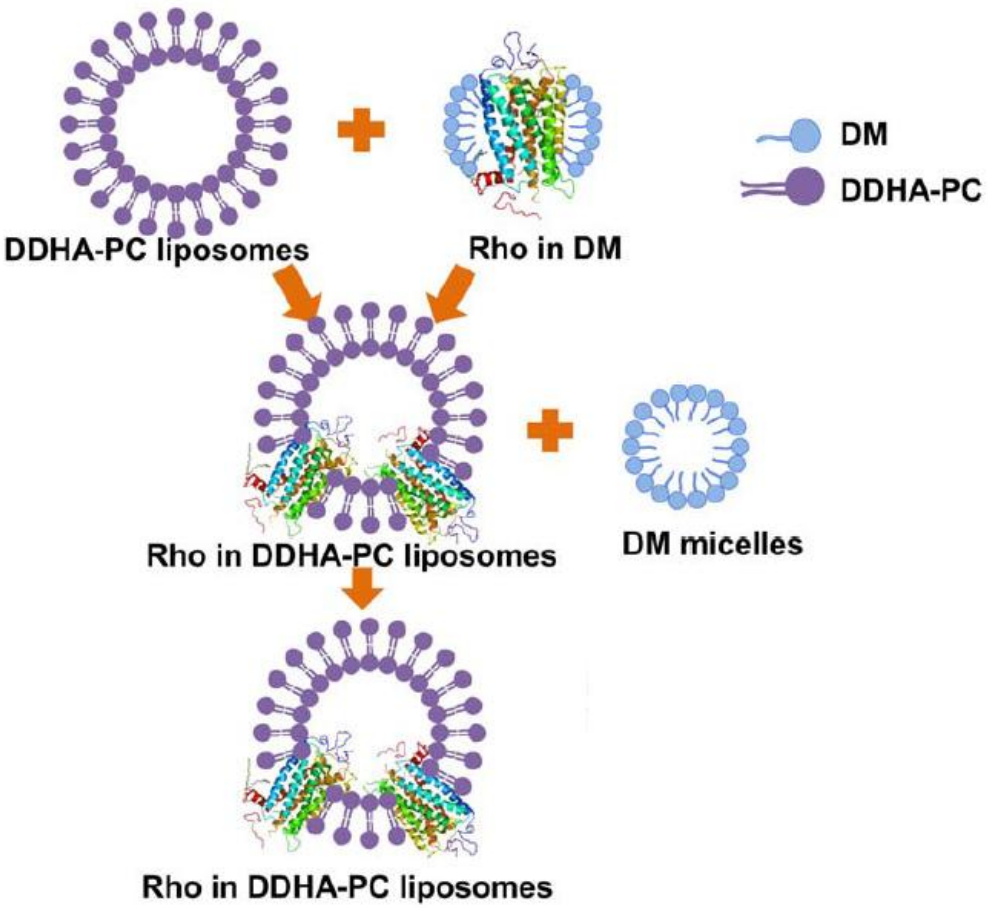

Graphical abstract

Highlights

- DDHA-PC liposomes stabilize the G90V rhodopsin mutation
- The liposome system allows retinal binding only for G90V but not for N55K mutant
- G90V conformation is likely stabilized by interaction with DHA fatty acid
- DDHA-PC effects on rhodopsin mutants associated with different RP clinical phenotypes